Journal of
Materials Chemistry C

PAPER

View Article Online
View Journal | View Issue

Cite this: J. Mater. Chem. C, 2015, 3, 3599

An ABA triblock copolymer strategy for intrinsically stretchable semiconductors†

Rui Peng,[a] Bo Pang,[a] Daqing Hu,[a] Mengjie Chen,[a] Guobing Zhang,[a] Xianghua Wang,[a] Hongbo Lu,[ab] Kilwon Cho[c] and Longzhen Qiu*[ab]

Received 30th October 2014,
Accepted 19th February 2015

DOI: 10.1039/c4tc02476a

www.rsc.org/MaterialsC

A novel semiconductor–rubber–semiconductor (P3HT–PMA–P3HT) triblock copolymer has been designed and prepared according to the principle of thermoplastic elastomers. It behaves as a thermoplastic elastomer with a Young's modulus (E) of 6 MPa for an elongation at break of 140% and exhibits good electrical properties with a carrier mobility of 9×10^{-4} cm^2 V^{-1} s^{-1}. This novel semiconductor may play an important role in low-cost and large-area stretchable electronics.

1 Introduction

Conjugated polymers have attracted enormous interest because of their potential applications in organic photovoltaics (OPVs),[1–4] organic light-emitting diodes (OLEDs),[5,6] and organic field-effect transistors (OFETs).[7–9] Compared with their inorganic counterparts, conjugated polymers are much more flexible and suitable for fabricating revolutionary flexible electronic products which would be light in weight, bendable or foldable, and compatible to low-cost fabrication methods such as high-throughput printing processing. A large number of highly bendable polymer devices built on plastic or metal foils have been demonstrated with flexed radii as small as several millimeters.[10,11] However, the rigid planar-conjugated backbones and highly crystallized states of conjugated polymers will inhibit the molecular motion and make the materials stiff and brittle,[12,13] which could lead to malfunction of the electronic devices under flexure. Furthermore, realization of stretchability in electronics is motivated by a wide range of applications including wearable electronics, smart skins, artificial organs, and integrated robotic sensors.[14–16] Such devices require materials that can sustain large mechanical strain without the loss of their function. Various techniques have been developed to modify the mechanical properties of semiconductors, such as curved structures,[16] nanofibrillar networks[10] and microcracks.[13] In particular, Lipomi and coworkers systematically studied the effects of molecular structure including side chains,[17] segmentation on main chains[18] and additives[19] on the mechanical properties of conjugated polymers.

Conjugated block copolymers are promising molecular architectures because the physical and electrical properties of the copolymers can be fine-tuned either by changing the physical properties of the segments or by controlling the self-assembled nanostructures. Combining a conjugated polymer block with flexible insulating blocks has the potential to generate conjugated copolymers with excellent mechanical properties. There have been a large number of reports on the synthesis of block copolymers containing a conjugated segment.[20–32] For example, Muller *et al.*[21] reported that diblock copolymers of polyethylene (PE) and P3HT display outstanding flexibility and toughness with elongations at break exceeding 600%. However, the P3HT-*b*-PE copolymers show typical plastic characteristics and irreversible deformation under strain.

In this contribution, we conceptualize an unprecedented strategy to design and prepare semiconducting polymers with high elasticity according to the principle of ABA triblock copolymer thermoplastic elastomers (TPEs), such as polystyrene-*b*-polybutadiene-*b*-polystyrene (SBS) and polystyrene-*b*-polyisoprene-*b*-polystyrene (SIS). The elasticity of such TPEs is derived from a two-phase nanostructure comprising hard polystyrene domains acting as physical cross-links in a rubbery matrix (Fig. 1a). Inspired by this system, we hypothesize that a class of novel semiconducting TPEs can be achieved by using rigid semiconducting polymer chains as hard segments and rubbery chains such as polyacrylate or poly(butadiene) as soft segments. However, charge transport in these semiconducting TPEs is challenging as the semiconducting phase disperses as a minor component in the dielectric matrix and can hardly form a conducting active channel. To solve this problem, a key feature of our process is controlling

[a] Key Lab of Special Display Technology, Ministry of Education, National Engineering Lab of Special Display Technology, State Key Lab of Advanced Display Technology, Academy of Opto-Electronic Technology, Hefei University of Technology, Hefei, 230009, China. E-mail: lzhqiu@hfut.edu.cn
[b] Key Lab of Advanced Functional Materials and Devices, Anhui Province, School of Chemical Engineering, Hefei University of Technology, Hefei, 230009, China
[c] Department of Chemical Engineering, Pohang University of Science and Technology, Pohang, 790-784, Korea

† Electronic supplementary information (ESI) available. See DOI: 10.1039/c4tc02476a

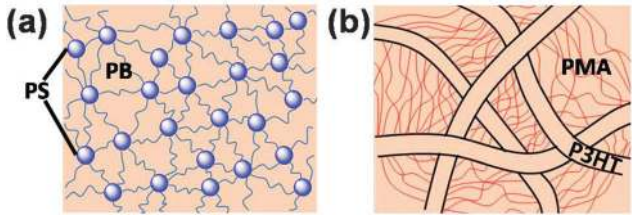

Fig. 1 Schematic illustration of (a) the structure of SBS, and (b) the structure of the P3HT-*b*-PMA-*b*-P3HT triblock copolymer.

the semiconducting component to form a nanofibrillar network with ordered molecular stacking embedded in the insulating polymer matrix (Fig. 1b). Our previous results have shown that the embedded nanofibrillar networks permit the reduction of the semiconductor content to a level as low as 3 wt% without considerable degradation of the field-effect characteristics.[33,34] If this architecture design indeed leads to the formation of semiconducting TPEs, it would provide a powerful platform for the preparation of a variety of semiconducting polymers with intrinsic stretchability.

2 Experimental

2.1 Materials

Diethyl *meso*-2,5-dibromoadipate and *N*,*N*,*N*′,*N*″,*N*″-pentamethyldiethylenetriamine (PMDETA) were obtained from TCI Co. Ltd., Shanghai, China. Other chemicals used in this work were purchased from Sigma-Aldrich Chemical Company, Sinopharm Chemical Reagent Co. Ltd., China. Methyl acrylate (MA) was passed through a column of basic alumina to remove the 4-methoxyphenol stabilizer. Chemical reagents were purchased and used as received. Tetrahydrofuran (THF) and toluene were freshly distilled over sodium wire under nitrogen prior to use.

2.2 Synthesis of PMA block (Br–PMA–Br) (1)

An oven-dried 100 ml flask was cooled under nitrogen and charged with diethyl *meso*-2,5-dibromoadipate (0.58 g, 1.61 mmol), methyl acrylate (10 g, 116.3 mmol), toluene (6 ml), PMDETA (0.28 g, 1.61 mmol) and a stir bar. The reaction mixture was purged with nitrogen for 30 min in an ice-bath, and CuBr (0.23 g, 1.61 mmol) was added. The flask was sealed with a rubber septum and warmed to room temperature. The reaction mixture was placed in an oil bath at 75 °C. After stirring the mixture for 4 h, the reaction was cooled to room temperature. The mixture was added to THF and passed through a neutral column (eluent = THF) to remove the residual catalyst. The solution was concentrated using a rotary evaporator. Afterward, it was precipitated into cold methanol to remove the residual monomer and other impurities. The polymer was dried under vacuum at 50 °C for 24 h (8.6 g, 86% yield). Data for PMA_{128}: GPC: $\overline{M_n}$ = 11.2 kDa, PDI=1.08. ^{1}H NMR (Fig. S1 in ESI,† $CDCl_3$, ppm): δ 4.25 (m, C*H*-Br), 4.13 (broad, OCH_2CH_3), 3.76 (m, $CHBrCOOCH_3$), 3.69 (s, CH_3O), 2.3 (broad, C*H* of polymer backbone), 1.94, 1.67, 1.51 (m, CH_2 of polymer backbone), 1.25 (t, OCH_2CH_3). FT-IR: $\nu_{C=O}$ = 1750 cm^{-1}.

2.3 Synthesis of PMA block (N_3–PMA–N_3) (2)

A round-bottomed glass flask (100 ml) with a magnetic bar was charged with Br–PMA–Br ($\overline{M_n}$ = 11.2 kDa, 5 g, 0.45 mmol), NaN_3 (0.29 g, 4.5 mmol) and DMF (40 ml). The resulting solution was stirred at room temperature for 24 h. After adding CH_2Cl_2 (200 ml) and water (200 ml), the organic phase was separated and washed with water (30 ml × 4), and then dried using Na_2SO_4. The solution was concentrated by a rotary evaporator. Afterward, it was precipitated into cold methanol to remove the residual DMF. The polymer was dried under vacuum at 50 °C for 24 h (4 g, 80% yield). GPC: $\overline{M_n}$ = 11.2 kDa, PDI = 1.08. ^{1}H NMR (Fig. S2 in ESI,† $CDCl_3$, ppm): δ 4.13 (broad, OCH_2CH_3), 3.93 (CH_2-N_3), 3.76 (m, CHN_3COOCH_3), 3.69 (s, CH_3O), 3.66 (broad, CH_3 of polymer backbone), 2.3 (broad, C*H* of polymer backbone), 1.94, 1.67, 1.51 (m, CH_2 of polymer backbone), 1.25 (t, OCH_2CH_3). FT-IR: $\nu_{C=O}$ = 1750 cm^{-1}. ν_{N3} = 2100 cm^{-1}.

2.4 Synthesis of ethynyl-terminated P3HT (P3HT-ethynyl) (3)

According to the literature,[20,23] in a typical experiment, an oven-dried two-necked glass flask (200 ml) was cooled under nitrogen and charged with 2,5-dibromo-3-hexylthiophene (4.36 g, 13.4 mmol), anhydrous THF (40 ml) and a magnetic stir bar. After adding *tert*-butylmagnesium chloride (13.4 ml, 1 M solution in THF), the reaction mixture was stirred at room temperature for 2 h. Subsequently, the mixture was diluted to 130 ml with anhydrous THF and Ni(dppp)Cl_2 (0.069 g, 0.127 mmol) was added. After 30 min, ethynylmagnesium bromide (2.5 ml, 0.5 M solution in THF) was added. After an additional 30 min, methanol was poured into the glass flask, which caused a dark-pure solid to precipitate. The desired P3HT was purified by a series of precipitations and dried under vacuum at room temperature (1.7 g, 40% yield). GPC: $\overline{M_n}$ = 5.6 kDa, PDI = 1.02. ^{1}H NMR (Fig. S3 in ESI,† $CDCl_3$, ppm): δ 6.98 (s, C*H* of the thiophene ring), 3.52 (s, CH of terminal ethynyl), 2.80 (t, $CH_2CH_2CH_2CH_2CH_2CH_3$), 1.71 (m, $CH_2CH_2CH_2CH_2$-CH_2CH_3), 1.50–1.30 (m, $CH_2CH_2CH_2CH_2CH_2CH_3$), 0.9 (t, CH_2CH_2-$CH_2CH_2CH_2CH_3$).

2.5 Synthesis of P3HT–PMA–P3HT triblock copolymer (4)

N_3–PMA–N_3 ($\overline{M_n}$ = 11.2 kDa, 0.5 g, 0.0455 mmol), P3HT-ethynyl ($\overline{M_n}$ = 5.6 kDa, 0.51 g, 0.0910 mmol) and PMDETA (0.016 g, 0.0910 mmol) were dissolved in anhydrous THF. The resulting solution was purged with nitrogen for 40 min in an ice-bath, subsequently CuBr (0.014 g, 0.0910 mmol) was added under nitrogen. The reaction mixture was placed in an oil bath at 50 °C for 3 days and taken out of the oil bath to cool to room temperature. The solution was diluted with THF and passed through a neutral column (eluent = THF) to remove residual catalyst, then concentrated using a rotary evaporator to afford the crude product. The desired polymers were confirmed by H NMR and GPC. GPC: $\overline{M_n}$ = 19 kDa, PDI = 1.12. ^{1}H NMR ($CDCl_3$, ppm): 7.43 (s, C*H* of triazole rings), 6.98 (s, C*H* of the thiophene ring), 4.13 (broad, OCH_2CH_3), 3.66 (broad, OCH_3), 2.80 (t, $CH_2CH_2CH_2CH_2CH_2CH_3$), 2.3 (broad, C*H* of poly(methyl acrylate) block), 1.94 (broad, CH_2CH of poly(methyl acrylate) block),

1.71 (m, $CH_2CH_2CH_2CH_2CH_2CH_3$), 1.50–1.30 (m, CH_2CH_2-$CH_2CH_2CH_2CH_3$).

2.6 Fabrication and characterization of field-effect transistors

Heavily n-doped Si wafer with 300 nm thermally grown SiO_2 surface layer (capacitance of 10.8 nF cm^{-2}) was employed as the substrate for the fabrication of OFETs. The n-type Si wafer serves as the common gate electrode and the SiO_2 layer acts as the gate dielectric. Prior to the modification of the SiO_2 layer with octadecyltrichlorosilane (ODTS), the wafer was cleaned in piranha solution (70 vol% H_2SO_4 + 30 vol% H_2O_2) for 30 min at 100 °C and washed with copious amounts of distilled water. The ODTS self-assembled monolayers (SAMs) were prepared by dipping the cleaned wafer into a 0.1 M toluene solution of ODTS for 2 h. A chloroform solution containing the semiconductor polymer was dropped onto the ODTS-SAM modified wafer and spin-coated. The polymer films were subsequently annealed (100–200 °C) in nitrogen. Then Au source–drain electrodes were prepared by thermal evaporation. The OFET devices had a channel length (L) of 100 μm and channel width (W) of 1 mm. The electrical characteristics of the OFET devices were measured in accumulation mode using a Keithley 2400 instrument under ambient conditions. The mobility values were obtained by using the following equation used at saturation regime: $I_d = (W/2L)C_i\mu(V_g - V_{th})^2$, where W/L is the channel width/length, I_d is the drain current in the saturated regime, C_i is the capacitance of the SiO_2 gate dielectric, and V_{th} is the threshold voltage.

2.7 Instrumentation

Nuclear magnetic resonance (NMR) spectra were recorded on a Mercury plus 600 MHz machine. Gel permeation chromatography (GPC) analyses were performed on a Waters Series 1525 gel coupled with a UV-vis detector using tetrahydrofuran as eluent with polystyrene as standard. Polystyrene standards in the range of 4100 to 278 000 g mol^{-1} were used to calibrate the GPC. The flow rate for the GPC system was 1 ml min^{-1}. Differential scanning calorimetry (DSC) was performed on a TA instrument Q2000 in a nitrogen atmosphere. The sample (about 3.0 mg in weight) was first heated to 250 °C and held for 5 min to remove thermal history, followed by a cooling rate of 10 °C min^{-1} to −40 °C and then a heating rate of 10 °C min^{-1} to 250 °C in all cases. UV-vis absorption spectra were recorded on a Perkin Elmer model λ 20 UV-vis spectrophotometer. IR spectra were recorded using a Thermo Nicolet Spectrum Nicolet 67 system using KBr pellets. Atomic force microscopy (AFM) images were obtained using a Veeco Multimode V instrument. Tensile tests were performed at room temperature on rectangular samples (20 mm × 5 mm × 1 mm) using a CMT4000 tensile machine, with a strain rate 2 mm min^{-1}.

3 Results and discussion

3.1 Synthesis and characterization

The synthesis route for the triblock copolymers is illustrated in Scheme 1. A novel semiconductor–rubber–semiconductor triblock copolymer, poly(3-hexylthiophene)–poly(methyl acrylate)–poly(3-hexylthiophene) (P3HT–PMA–P3HT), was synthesized *via* the "click" reaction of two ethynyl-terminated P3HT (P3HT–C≡CH) chains and an α,ω-diazido-terminated poly(methyl acrylate) (N_3–PMA–N_3). Well-fined N_3–PMA–N_3 was synthesized *via* Cu-mediated atom transfer radical polymerization of methyl acrylate initiated by diethyl *meso*-2,5-dibromoadipate, followed by displacement of the bromide end-group with azides using NaN_3 in DMF at room temperature. Monomodal P3HT–C≡CH was prepared *via* a Ni-catalyzed Grignard metathesis (GRIM) polymerization and purified according to literature procedures.[35] N_3–PMA–N_3

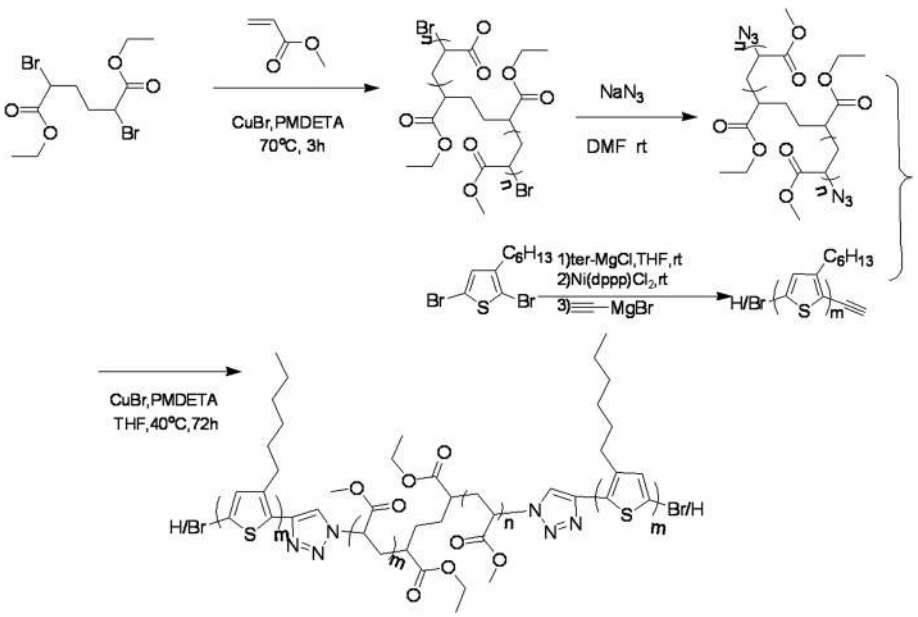

Scheme 1 Synthesis route for P3HT-*b*-PMA-*b*-P3HT triblock copolymer.

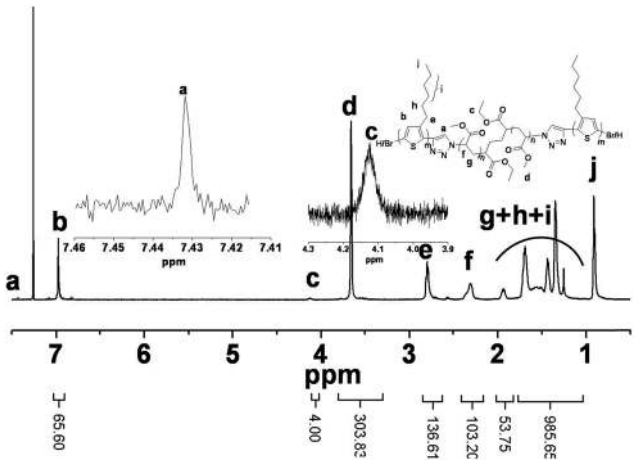

Fig. 2 The ^{1}H NMR spectrum of P3HT-*b*-PMA-*b*-P3HT triblock copolymer (**P3**).

was reacted with 2 equiv. of P3HT–C≡CH using *N*,*N*,*N*′,*N*″,*N*″-pentamethyldiethylenetriamine (PMDETA)/CuBr as the catalyst system at 40 °C in tetrahydrofuran (THF). After filtering the resulting reaction mixture through neutral alumina to remove the catalyst, the crude P3HT–PMA–P3HT triblock copolymers were obtained by precipitating the reaction mixtures in methanol.

As shown in Fig. 2, ^{1}H-NMR spectroscopy was used to determine the structures of the triblock copolymers. The absence of the starting P3HT–C≡CH and N_3–PMA–N_3 was confirmed by the disappearance of both resonances corresponding to the alkynyl groups at δ = 3.52 ppm and the azide moiety at δ = 3.9 ppm. The formation of the triazole rings was confirmed by the presence of a new resonance at δ = 7.43 ppm[20] and the disappearance of the diagnostic ν_{N3} IR signal (Fig. S4 in ESI†). Moreover, after purification *via* gel permeation chromatography (GPC), a triblock copolymer composed of two rodlike 5600 g mol^{-1} rr-P3HT chains covalently linked to a 11 200 g mol^{-1} PMA coil polymer with an overall number-average molecular weight of 19 000 g mol^{-1} was obtained (see Fig. 3a and b). Notably, a small shoulder appeared in the GPC trace of the crude triblock copolymers since P3HT with alkyne end groups could not reach 100% conversion.[36,37] However, the limited portion of P3HT homopolymer in the triblock copolymer has no influence on the electrical and mechanical performance, because P3HT can self-assemble into well-ordered nanowires acting as charge transport channels.

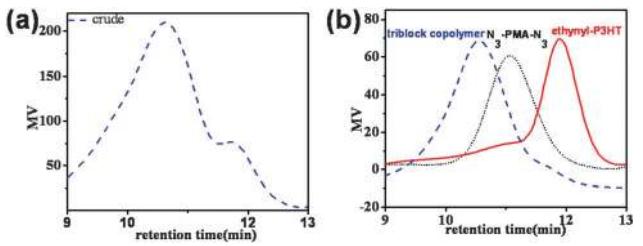

Fig. 3 Representative GPC trace of the crude product (a, blue line) and highly purified triblock copolymers (b, blue line), poly(methyl acrylate) homopolymer (b, black line) and P3HT homopolymer (b, red line).

The chemical compositions of the four triblock copolymers derived from P3HT and PMA segments of different molecular weights are summarized in Table 1.

3.2 Optical properties

UV-visible absorbance spectra, which were referenced to the extended triblock and collapsed triblock, were collected in dilute chloroform solution and solid state film forms. In Fig. 4 (red line), the triblock exhibited a broad absorption peak centered at 455 nm, which corresponded to the π–π* electronic transition of the triblock copolymer in solution. This phenomenon resembled the characteristic of highly rr-P3HT. The black line represents the collapsed triblock, a broad π–π* electronic transition band was evident with a peak centered at 518 nm and two additional vibronic structures at 548 nm and 605 nm which were interpreted as the coupling of the C=C double bond symmetric stretch and the π–π* electronic transition. The large red shift (about 70 nm) between solution and solid state films indicates the presence of strong intermolecular interactions and the planarization effect of the conjugated polymer backbone. The results suggest that intermolecular interactions are relatively strong in favor of the mobility.

3.3 Thermal and mechanical properties

The thermal behavior of the P3HT-*b*-PMA-*b*-P3HT triblock copolymer was investigated by differential scanning calorimetry (DSC) (Fig. 5). The DSC trace of P3HT-*b*-PMA-*b*-P3HT triblock copolymer was typical of an immiscible system. The result was in agreement with the obvious difference in solubility between P3HT (13.1 (MPa)$^{1/2}$)[38] and PMA (20.7 (MPa)$^{1/2}$),[39] which provides a strong driving force for phase separation. It showed a glass transition at 2 °C corresponding to the T_g of the PMA phase and an endotherm peak at 200 °C corresponding to T_m of the P3HT phase. The T_g of PMA segments and the T_m of P3HT segments in triblock copolymer were lower than those of PMA (10 °C)[40] and P3HT (215.6 °C)[41] homopolymers because of their relatively low molecular weight.

Although the starting N_3–PMA–N_3 is viscous and P3HT–C≡CH is brittle at room temperature, the P3HT-*b*-PMA-*b*-P3HT triblock copolymers have excellent mechanical properties. The film of **P4** can be elastically deformed as displayed in the insert of Fig. 6. The strain–stress curve indicates a Young's modulus (E) of 6 MPa, an elongation at break (ε) of 140% and a true stress at break [$\sigma_t = \sigma(1 + \varepsilon/100)$] (here, σ is the maximum stress at break) of 1.4 MPa. Compared with E of 28 MPa, ε of 13% and σ_t of 4 MPa for the P3HT homopolymer reported in the literature,[21] the modulus became lower and the elongation became larger, which are typical characteristics of a plastic-to-rubber transition. It should be noted that the mechanical properties of P3HT are highly dependent on the measuring method. For instance, O'Connor[12] and Lipomi[42] reported the modulus of P3HT films was 0.25 GPa and 0.92 GPa using a buckling-based metrology. The reason may be that the buckling-based technique measured the in-plane elastic modulus, and the anisotropic microstructure of the films may lead to an anisotropic elastic modulus. For comparison, we used the data of bulk

Table 1 Compositions of P3HT-*b*-PMA-*b*-P3HT

Polymer	P3HT block (NMR)	PMA block (NMR)	P3HT (wt%)	P3HT block (GPC)	PMA block (GPC)	$\overline{M_n}$ (GPC)	PDI (GPC)
$P3HT_1$	3800	—	100	5200	—	—	1.04
$P3HT_2$	6600	—	100	5600	—	—	1.02
P1	3800	11 000	41	5200	11 200	19 000	1.29/1.12[a]
P2	3800	24 000	24	5200	14 000	26 000	1.38
P3	6600	11 000	55	5600	11 200	16 000	1.51
P4	6600	24 000	35	5600	14 000	27 000	1.64

[a] The PDI of sampled purified by GPC.

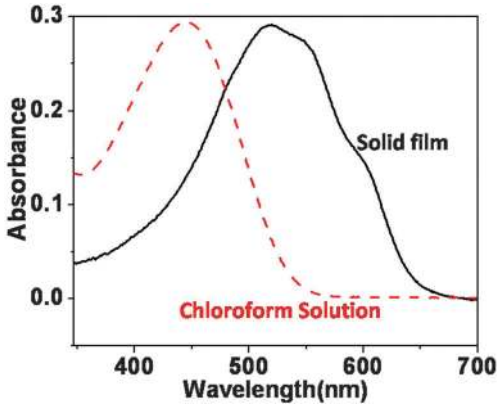

Fig. 4 UV-vis absorption spectra of P3HT-*b*-PMA-*b*-P3HT in chloroform solution and in thin film form.

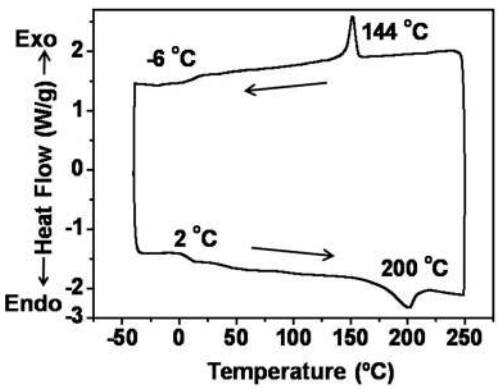

Fig. 5 The DSC trace of P3HT–PMA–P3HT triblock copolymer.

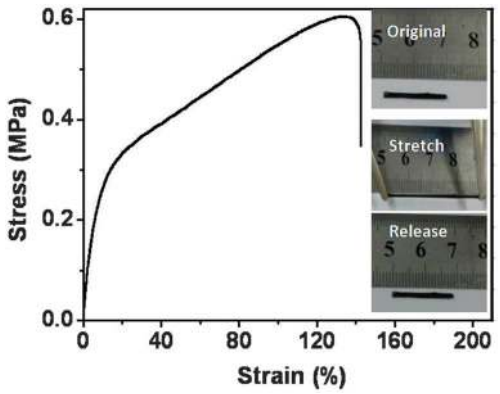

Fig. 6 The strain–stress profile of P3HT–PMA–P3HT triblock copolymer.

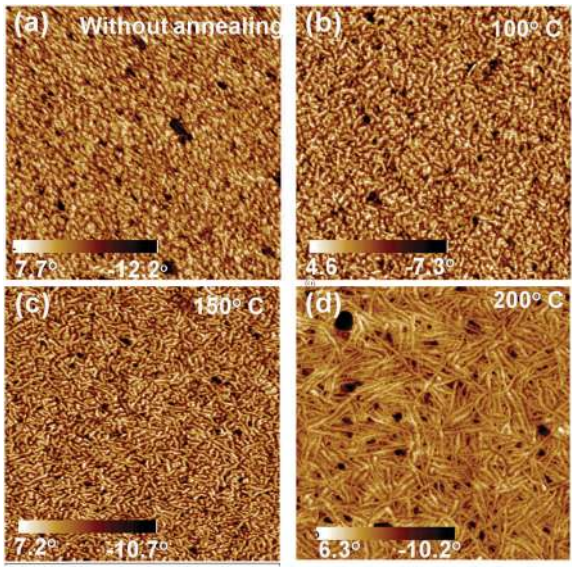

Fig. 7 AFM topography images of P3HT–PMA–P3HT at different annealing temperatures.

samples obtained from a similar measurement technique. Furthermore, the mechanical properties of our triblock copolymer could be improved by increasing the molecular weight of the soft PMA block.

3.4 The film morphologies and microstructure

Film morphology and crystallinity play important roles in OFET device performance. Atomic force microscopy (AFM) was applied to investigate the morphology of **P4** films annealed at different temperatures for 15 min (Fig. 7). The AFM phase image of an as-prepared film without any thermal annealing shows a granular phase pattern. As the annealing temperature increased, the granular domains are elongated. When annealed at 200 °C, the AFM images showed clear evidence of nanofibrillar structures with lengths of several hundred nanometers and widths of about 10 nm. Considering the PMA is in a rubbery state, the nanofibrillar structures can be attributed as a result of π–π stacking of P3HT segments. The P3HT nanofibers with high aspect ratios can keep the connectivity of the semiconducting layers in the block copolymer films and thus play a significant role in achieving effective charge transport.[43]

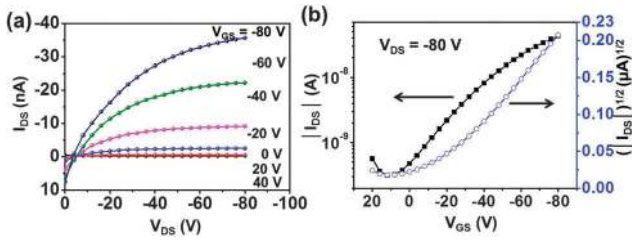

Fig. 8 Field-effect characteristics of top contact OFETs based on **P4**: (a) output and (b) transfer.

3.5 OFET characterization

OFETs device with bottom-gate and top-contact geometry were used to investigate the field-effect mobility of P3HT-*b*-PMA-*b*-P3HT triblock copolymers. Fig. 8 shows the typical field-effect transistor characteristics of **P4** measured in accumulation mode under ambient conditions. The devices were found to be well-behaved p-type transistors with a clear linear regime at small source–drain voltages and a saturation regime at V_{DS} values higher than the gate voltage. Table 2 summarizes the device parameters for all of the polymers. The homo P3HT films with molecular weights of 3.8 and 6.6 kg mol^{-1} (NMR) showed carrier mobilities of 1.7 × 10^{-4} and 2.4 × 10^{-4} cm^2 V^{-1} s^{-1} (Fig. S5 in ESI†), respectively. The poor mobilities observed in our work are attributed to the low molecular weight of P3HT and are comparable with those of P3HT with similar molecular weight reported in literature.[37] The field-effect performances of triblock copolymers are highly dependent on the content of P3HT segments. **P1** (41% P3HT) and **P3** (55% P3HT) with relatively high contents of P3HT displayed enhanced mobilities of 3.5 × 10^{-4} and 3.0 × 10^{-4} cm^2 V^{-1} s^{-1}, respectively, compared to their P3HT homopolymers. The enhancement of charge transport properties was also reported in poly(3-hexylthiophene)-*b*-polystyrene diblock copolymers and was ascribed to the highly crystalline, ordered P3HT domains in the copolymer films.[43] The mobility of the triblock copolymers decreased with higher PMA content because the PMA segment is an insulator. The maximum carrier mobility was 9 × 10^{-4} cm^2 V^{-1} s^{-1} for the **P3** film.

Table 2 Summary of all field-effect mobilities of rr-P3HT and the triblock copolymers

Polymer	Mobility (cm^2 V^{-1} s^{-1})	Max mobility (cm^2 V^{-1} s^{-1})	On/off ratio	Threshold voltage
P3HT$_1$	1.5 × 10^{-4}	4.2 × 10^{-4}	33	17.6
P3HT$_2$	2.4 × 10^{-4}	4.5 × 10^{-4}	207	17.3
P1	3.5 × 10^{-4}	4.3 × 10^{-4}	166	4.9
P2	9.9 × 10^{-5}	1.1 × 10^{-4}	175	7.2
P3	3.0 × 10^{-4}	9.0 × 10^{-4}	246	−10.7
P4	1.7 × 10^{-4}	2.1 × 10^{-4}	666	−8.6

The change of electrical properties of **P4** film under stress was evaluated using a transfer process as illustrated in Fig. 9a. The **P4** film was firstly spin coated onto a PDMS substrate, followed by straining to a certain elongation. Then the film was transferred to a silicon substrate with pre-defined source and drain electrodes in the tensile state. Fig. 9b shows the change of mobility as a function of strain. The on-current slowly decreased up to an elongation of 20%. After that, a considerable decrease was observed for the elongation range from 40% to 60%. Though the mobility monotonously decreased as the elongation increased, the film with 60% elongation still showed field-effect performance and the mobility was 10% of the film without any strain. Fig. 9d shows the change in transfer curves measured in a stretch cycle at a strain of 40%. When the **P4** sample was stretched to 40% and released to 0%, the on-current irreversibly decreased to about 50% of the pristine state. This decrease may be caused by the non-optimized phase structure of the films. Further study will be conducted to improve this aspect.

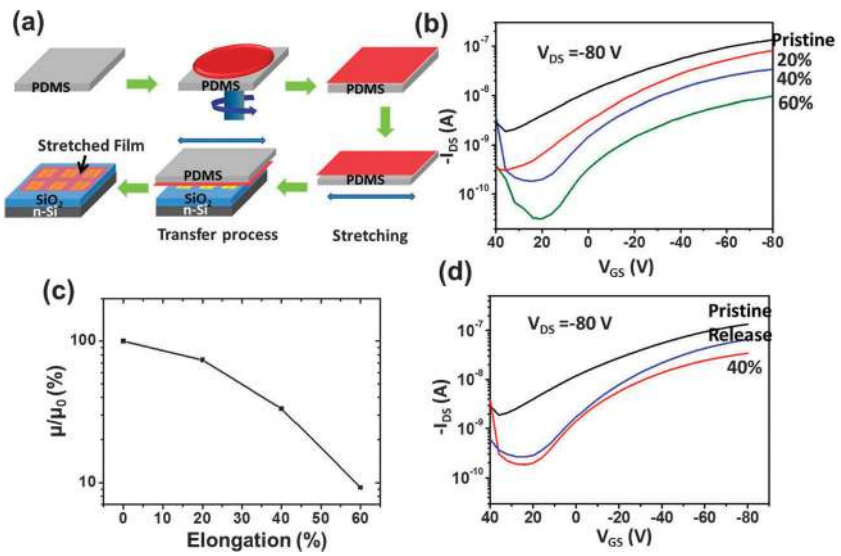

Fig. 9 (a) Schematic illustration of the steps used to measure the mobility under stress. (b) Change of the transfer curves at different strains. (c) The corresponding change of mobility as a function of strain. (d) Change of the transfer curves during a stretching cycle at a strain of 40%.

4 Conclusions

In conclusion, novel copolymers based on amorphous PMA blocks and two crystalline P3HT blocks were successfully synthesized *via* coupling of the alkyne-terminated P3HT with the diazide-terminated PMA using a click reaction. These triblock copolymers behaved as thermoplastic elastomers with a Young's modulus (E) of 6 MPa for an elongation at break of 140%. The spin-cast triblock copolymer films were found to self-assemble into well ordered nanofibrillar structures under thermal annealing, which is optimal for charge transfer in field-effect transistors. A maximum saturated hole mobility of 9×10^{-4} cm^2 V^{-1} s^{-1} was obtained for P3HT-*b*-PMA-*b*-P3HT triblock copolymer containing 55 wt% P3HT. The semiconductor–rubber–semiconductor (SRS) structure would have a significant impact on the next generation of stretchable electronics.

Acknowledgements

This research was supported by National Basic Research Program of China (Grant No. 2012CB723406), National Natural Science Foundation of China (Grant No. 61107014, 51203039, 21204017, 21174036, 51103034), Program for New Century Excellent Talents in University (Grant No. NCET-12-0839).

Notes and references

1 J. B. You, L. T. Dou, K. Yoshimura, T. Kato, K. Ohya, T. Moriarty, K. Emery, C. C. Chen, J. Gao, G. Li and Y. Yang, *Nat. Commun.*, 2013, **4**, 1446.
2 H. X. Zhou, L. Q. Yang and W. You, *Macromolecules*, 2012, **45**, 607.
3 H. L. Yip and A. K. Y. Jen, *Energy Environ. Sci.*, 2012, **5**, 5994.
4 J. W. Chen and Y. Cao, *Acc. Chem. Res.*, 2009, **42**, 1709.
5 M. C. Gather, A. Kohnen and K. Meerholz, *Adv. Mater.*, 2011, **23**, 233.
6 S. Reineke, F. Lindner, G. Schwartz, N. Seidler, K. Walzer, B. Lussem and K. Leo, *Nature*, 2009, **459**, 234.
7 T. Lei, J.-H. Dou, X.-Y. Cao, J.-Y. Wang and J. Pei, *J. Am. Chem. Soc.*, 2013, **135**, 12168.
8 P. Sonar, T. R. B. Foong, S. P. Singh, Y. Li and A. Dodabalapur, *Chem. Commun.*, 2012, **48**, 8383.
9 J. Li, Y. Zhao, H. S. Tan, Y. Guo, C.-A. Di, G. Yu, Y. Liu, M. Lin, S. H. Lim, Y. Zhou, H. Su and B. S. Ong, *Sci. Rep.*, 2012, **2**, 754.
10 M. Kaltenbrunner, T. Sekitani, J. Reeder, T. Yokota, K. Kuribara, T. Tokuhara, M. Drack, R. Schwodiauer, I. Graz, S. Bauer-Gogonea, S. Bauer and T. Someya, *Nature*, 2013, **499**, 458.
11 G. H. Gelinck, H. E. A. Huitema, E. Van Veenendaal, E. Cantatore, L. Schrijnemakers, J. Van der Putten, T. C. T. Geuns, M. Beenhakkers, J. B. Giesbers, B. H. Huisman, E. J. Meijer, E. M. Benito, F. J. Touwslager, A. W. Marsman, B. J. E. Van Rens and D. M. De Leeuw, *Nat. Mater.*, 2004, **3**, 106.
12 B. O'Connor, E. P. Chan, C. Chan, B. R. Conrad, L. J. Richter, R. J. Kline, M. Heeney, I. McCulloch, C. L. Soles and D. M. DeLongchamp, *ACS Nano*, 2010, **4**, 7538.
13 A. Chortos, J. Lim, J. W. F. To, M. Vosgueritchian, T. J. Dusseault, T.-H. Kim, S. Hwang and Z. Bao, *Adv. Mater.*, 2014, **26**, 4253.
14 D. J. Lipomi, M. Vosgueritchian, B. C. K. Tee, S. L. Hellstrom, J. A. Lee, C. H. Fox and Z. N. Bao, *Nat. Nanotechnol.*, 2011, **6**, 788.
15 T. Sekitani, H. Nakajima, H. Maeda, T. Fukushima, T. Aida, K. Hata and T. Someya, *Nat. Mater.*, 2009, **8**, 494.
16 D. Y. Khang, H. Q. Jiang, Y. Huang and J. A. Rogers, *Science*, 2006, **311**, 208.
17 D. J. Lipomi, H. Chong, M. Vosgueritchian, J. Mei and Z. Bao, *Sol. Energy Mater. Sol. Cells*, 2012, **107**, 355.
18 S. Savagatrup, A. S. Makaram, D. J. Burke and D. J. Lipomi, *Adv. Funct. Mater.*, 2014, **24**, 1169.
19 A. D. Printz, S. Savagatrup, D. J. Burke, T. N. Purdy and D. J. Lipomi, *RSC Adv.*, 2014, **4**, 13635.
20 M. Urien, H. Erothu, E. Cloutet, R. C. Hiorns, L. Vignau and H. Cramail, *Macromolecules*, 2008, **41**, 7033.
21 C. Muller, S. Goffri, D. W. Breiby, J. W. Andreasen, H. D. Chanzy, R. A. J. Janssen, M. M. Nielsen, C. P. Radano, H. Sirringhaus, P. Smith and N. Stingelin-Stutzmann, *Adv. Funct. Mater.*, 2007, **17**, 2674.
22 R. Duan, L. Ye, X. Guo, Y. Huang, P. Wang, S. Zhang, J. Zhang, L. Huo and J. Hou, *Macromolecules*, 2012, **45**, 3032.
23 Z. Q. Wu, R. J. Ono, Z. Chen and C. W. Bielawski, *J. Am. Chem. Soc.*, 2010, **132**, 14000.
24 H. C. Moon, A. Anthonysamy, Y. Lee and J. K. Kim, *Macromolecules*, 2010, **43**, 1747.
25 Q. Zhang, A. Cirpan, T. P. Russell and T. Emrick, *Macromolecules*, 2009, **42**, 1079.
26 S. P. Wu, L. J. Bu, L. Huang, X. H. Yu, Y. C. Han, Y. H. Geng and F. S. Wang, *Polymer*, 2009, **50**, 6245.
27 C.-A. Dai, W.-C. Yen, Y.-H. Lee, C.-C. Ho and W.-F. Su, *J. Am. Chem. Soc.*, 2007, **129**, 11036.
28 J. Liu, E. Sheina, T. Kowalewski and R. D. McCullough, *Angew. Chem., Int. Ed.*, 2002, **41**, 329.
29 M. C. Stefan, M. P. Bhatt, P. Sista and H. D. Magurudeniya, *Polym. Chem.*, 2012, **3**, 1693.
30 M. C. Iovu, M. Jeffries-El, E. E. Sheina, J. R. Cooper and R. D. McCullough, *Polymer*, 2005, **46**, 8582.
31 M. Sommer, A. S. Lang and M. Thelakkat, *Angew. Chem., Int. Ed.*, 2008, **47**, 7901.
32 K. Palaniappan, N. Hundt, P. Sista, H. Nguyen, J. Hao, M. P. Bhatt, Y. Y. Han, E. A. Schmiedel, E. E. Sheina and M. C. Biewer, *J. Polym. Sci., Part A: Polym. Chem.*, 2011, **49**, 1802.
33 L. Z. Qiu, X. Wang, W. H. Lee, J. A. Lim, J. S. Kim, D. Kwak and K. Cho, *Chem. Mater.*, 2009, **21**, 4380.
34 G. H. Lu, H. W. Tang, Y. P. Qu, L. G. Li and X. N. Yang, *Macromolecules*, 2007, **40**, 6579.
35 Z. Li, R. J. Ono, Z.-Q. Wu and C. W. Bielawski, *Chem. Commun.*, 2011, **47**, 197.
36 R. H. Lohwasser and M. Thelakkat, *Macromolecules*, 2012, **45**, 3070.
37 R. J. Kline, M. D. McGehee, E. N. Kadnikova, J. S. Liu, J. M. J. Frechet and M. F. Toney, *Macromolecules*, 2005, **38**, 3312.

38 J. Jaczewska, I. Raptis, A. Budkowski, D. Goustouridis, J. Raczkowska, A. Sanopoulou, E. Pamula, A. Bernasik and J. Rysz, *Synth. Met.*, 2007, **157**, 726.
39 J. E. Mark, *Physical Properties of Polymer Handbook*, Springer, New York, 2nd edn, 2007.
40 *Polymer Handbook*, ed. I. Brandrup, E. H. Immergut and E. A. Grulke, John Wiley & Sons, New York, 4th edn, 1999.
41 H. C. Yang, T. J. Shin, L. Yang, K. Cho, C. Y. Ryu and Z. N. Bao, *Adv. Funct. Mater.*, 2005, **15**, 671.
42 S. Savagatrup, E. Chan, S. M. Renteria-Garcia, A. D. Printz, A. V. Zaretski, T. F. O'Connor, D. Rodriquez, E. Valle and D. J. Lipomi, *Adv. Funct. Mater.*, 2015, **25**, 427.
43 X. Yu, K. Xiao, J. H. Chen, N. V. Lavrik, K. L. Hong, B. G. Sumpter and D. B. Geohegan, *ACS Nano*, 2011, **5**, 3559.

